Rapid Methodology for Design and Performance Prediction of Integrated Supersonic Combustion Ramjet Engine

Hideo Ikawa*
Northrop Corporation, Hawthorne, California 90250

The design integration of a supersonic combustion ramjet engine (SCRAMJET) with an airframe dictates the mission success of transatmospheric or hypersonic cruise vehicles. Special interest must be given for the hypersonic atmospheric boost phase of the mission where most of the propulsive energy is expended. For this purpose, the operational efficiency is established by the effective specific impulse and the thrust to weight ratio of the accelerating vehicle. In order to analyze the foregoing problems, a methodology is developed, which permits a quick performance evaluation of an idealized, integrated SCRAMJET vehicle for preliminary design analysis. The capabilities of methodology are 1) designing an integrated vehicle consisting of the forebody inlet, supersonic flow combustor and afterbody expansion nozzle; 2) generating the design and off-design performance data; and 3) performing many design iterations for tradeoff studies. Samples of the design and off-design performance analysis of generic hypersonic vehicles are presented. The methodology is suitable to be programmed and executed on a personal computer.

Nomenclature

A	= combustor cross-sectional area
Ac_∞	= freestream capture area
a,b	= parameters defined by Eq. (4)
C	= Chapman-Rubesin viscosity law
Cd, Cl, Cm	= drag, lift, and pitching moment coefficients
Ct	= thrust coefficient
Cp	= pressure coefficient; specific heat of air/gas
D, L, M	= drag, lift, and pitching moment
F, F_0, F_1	= parameters defined by Eq. (6)
Fm, Gm, Hm	= parameters defined by Eq. (4)
f	= fuel/air mass flux ratio
g	= gravitational constant
H_f	= heat content of fuel
Hc	= inlet height of combustor
h	= altitude; specific enthalpy
ISP	= propulsive or system specific impulse
ISP_{eff}	= effective specific impulse, $ISP(1 - D/Th)$
kc	= combustor divergent parameter defined by Eq. (3)
LB_f	= forebody length from nose to cowl lip
LH_2	= liquid hydrogen fuel
M	= Mach number
m	= mass of air or fuel
$\dot{m}$	= mass flux
p	= static pressure
p_t	= total pressure
Q_f	= heat parameter defined by Eq. (12)
q_∞	= dynamic pressure
Rex	= Reynolds number with respect to length
Sh_i	= shock positions, $i = 1, 2, 3 \ldots$
T	= air/gas static temperature
T_t	= air/gas total temperature
Th	= thrust
u	= flow velocity
V	= vehicle velocity
x	= longitudinal length
α	= angle of attack
α,β,Γ	= parameters defined by Eq. (7)
γ	= ratio of specific heat
δ	= surface deflection angle
θ	= shock angle
ϕ	= fuel/air equivalence ratio ($\phi = 1$, stoichiometric)
λ	= stoichiometric fuel/air mixture ratio (1/34 for LH_2)
η	= combustor efficiency factor
$\bar{\chi}$	= viscous interaction parameter, $M_\infty^3(C/Rex)^{1/2}$
ν	= Prandtl-Meyer angle

Subscripts

a	= air
c	= combustor
e	= combustor exit
f	= fuel
fb	= forebody
i	= combustor inlet
n	= nozzle
p	= propulsive
t	= stagnation flow property
∞	= freestream flow property

Presented as Paper 89-2682 at the AIAA/ASME/SAE/ASEE 25th Joint Propulsion Conference, Monterey, CA, July 10–12, 1989; received July 17, 1989; revision received Dec. 29, 1989.

*Senior Technical Specialist, Aircraft Division. Member AIAA.

Introduction

A VIABLE development of transatmospheric (TAV) or hypersonic (HV) vehicles depends upon the successful integration of a supersonic combustion ramjet engine (SCRAMJET) with the vehicle. Mission success of a TAV during the hypersonic boost phase can be dictated by the operational efficiency of the accelerating vehicle system. Furthermore, establishment of an operational flight corridor requires a compromise among airbreathing engine performance, vehicle aerodynamic performance, and structural thermal load limit resulting from aeroheating.

The SCRAMJET system analysis is complicated because it requires the understanding of many complex phenomena.[1-4] Detailed analyses of the SCRAMJET concept are being pursued by many computational fluid dynamics (CFD) researchers, and their work is well summarized by White et al.[1] However, CFD analysis is too complex and costly to apply

for the preliminary design evaluations of the integrated SCRAMJET vehicle configuration.

The objective of the present study was to develop a performance prediction methodology that permits a quick evaluation of an idealized, integrated SCRAMJET vehicle during the preliminary design stage. The methodology must be capable of 1) designing an integrated SCRAMJET vehicle for prescribed geometrical constraints and for a given design flight condition; 2) generating the design and off-design performance data; and 3) performing many design iterations quickly and economically for trade studies. For simplicity, the methodology development presented herein is based upon a *two-dimensional, inviscid flow analysis*. Implications of viscous interaction (VI) effects will be discussed, but the VI effects are not implemented in the prototype SCRAMJET prediction program. The methodology has been translated into BASICA computer language and can be executed quickly and economically on an IBM personal computer (PC). The program can either be used as a stand-alone code or as a SCRAMJET module in a trajectory simulation program.

Methodology Development

Integrated Forebody Surface/SCRAMJET Inlet Analysis

At hypersonic speed, the displacement angle of the bow shock wave emanating from the nose of the vehicle is very small (within a few degrees). This fact combined with the mass flow requirement of the SCRAMJET engine can cause the longitudinal length of the external wedge or conical compression device to become very large. In order to optimize the SCRAMJET performance and to keep the overall vehicle length to a minimum, it has been suggested that the lower surface of the vehicle forebody be integrated to form part of the external compression device.[4] For the purpose of preliminary design analysis, the forebody compression surfaces are modeled as a two-dimensional multiramp wedge. The behavior of the flowfield through shock waves is described using inviscid oblique shock theory. The effect of displacement thickness and friction as a result of viscous flow interaction will be briefly discussed later.

The geometry of the forebody compression surface is designed so as to capture 100% of the freestream air mass flow at an arbitrarily selected design flight condition. Parameters that define the design flight condition are Mach number, angle of attack (AOA), and altitude. There are several ways the geometry can be specified. They are 1) the slope of each ramp on the wedge and the longitudinal distance between the vehicle nose and the inlet lip of the cowl are given; 2) a mass flow requirement and the distance between the nose and cowl inlet position are given; or 3) a mass flow requirement and an initial ramp angle are given. For designs having a constrained forebody length, the vertical position of the cowl is adjusted so the bow shock wave intercepts the cowl lip. The subsequently downstream ramp positions are longitudinally adjusted so as to make all the shock waves generated by the multiramp wedge coalesce and intercept the cowl lip (see Fig. 1).

The strength of the bow shock is dependent upon the total compression angle measured relative to the freestream. This angle includes the initial ramp deflection and angle of attack. The greatest loss in total pressure occurs across the bow shock. Because of this, the overall total pressure recovery of the local flowfield may not be improved much by having a smooth isentropic compression downstream of the nose. For this reason and for analytic simplicity, a compression surface with three ramps appears to suffice for the forebody design analysis.

The subsequent internal compression processes downstream of the cowl inlet to the combustor inlet are tailored to align the final flow direction to be parallel with respect to the vehicle body coordinate system as shown by Sh_3 and Sh_4 in Fig. 1. The local flowfield properties (Mach numbers, mass flux, temperature, and pressure) defined at this point are used as the initial conditions for the subsequent combustor inlet analysis. Once the forebody inlet configuration is designed, the geometry will be fixed for any off-design point performance analysis.

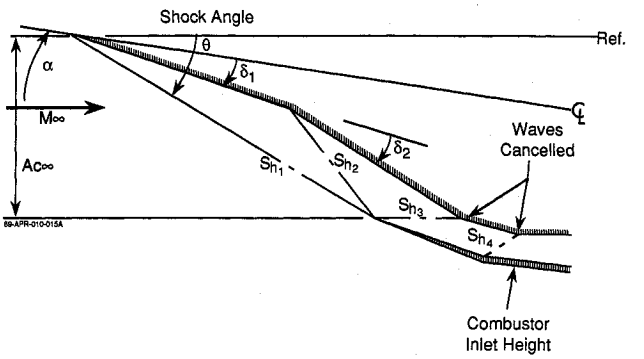

Fig. 1 Integrated forebody/inlet schematics.

Divergent Area Supersonic Combustor Analysis

Many complexities and uncertainties exist in the supersonic combustor design, for example, 1) the turbulent mixing process of fuel in a supersonic air stream; 2) the residence and reaction times of the fuel/air mixture that determine the supersonic combustor size; 3) the burning characteristics of the fuel/air mixture in an environment of high-speed (order of 3 km/s) and low-pressure (order of 0.1 atmosphere) flow; 4) the high-enthalpy flow contributing to the real-gas effects such as species dissociation of gas; 5) the chemical reaction of combusting media, etc. The CFD analyses are being pursued by many researchers to enhance the understanding of these complex phenomena.[1,2] However, these CFD approaches are costly and unsuitable for conducting preliminary design studies. To provide a more rapid, less costly alternative methodology for use in preliminary design analysis, an idealized supersonic combustor analytical model is derived. Essentially, all of these uncertainties about the combustion process are treated as if they exist in a "black box." Then engineering judgment is applied to establish a reasonable efficiency factor of energy conversion based upon the energy balance, i.e., the work exerted by the vehicle to the surrounding atmosphere is directly proportional to the available heat content of the fuel.

For a first-order approximation of the supersonic combustor analysis, an approach analagous to the constant area afterburner or the ramjet analysis[5,6] is applied. It is well known that heating of supersonic flow in a constant area channel results in a loss of the flow momentum from the inlet to the exit of the combustor. Because engine thrust is produced by positive momentum flux, this deficiency can be remedied by the divergent area combustor design (see Fig. 2) as shown by the velocity derivative[5] [Eq. (1)] and by the condition defined by Eq. (2)

$$\frac{du}{u} = \left(\frac{dA}{A} - \frac{dH_f}{CpT}\right)/(M^2 - 1) \tag{1}$$

For a desired $du/u > 0$, we must have

$$\frac{dA}{A} > \frac{dH_f}{CpT} \tag{2}$$

In order to avoid numerical integrations of a set of differential equations, a multiplying factor kc is introduced [Eq. (3)] to solve for the divergent channel flow problem

$$\frac{dA}{A} = kc\,\frac{dH_f}{CpT} \tag{3}$$

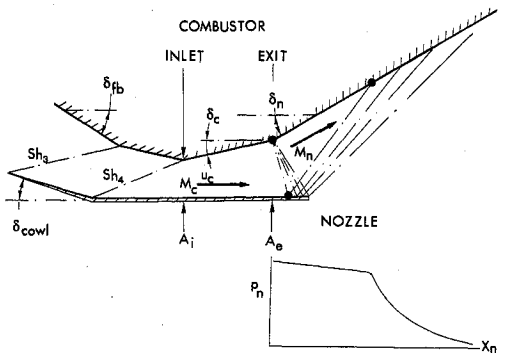

Fig. 2 Integrated combustor/afterbody nozzle schematics.

where

$kc = 0$: solution for a constant area flow
$0 < kc \leq = 1$: increasing area channel, decreasing momentum flux
$1 < kc$: increasing area channel, increasing momentum flux

For a constant value of kc, the flow parameters of a divergent area channel with heat addition can be derived in closed-form solutions as a function of Mach number and specific heat ratio, similar to the ones given for the constant area channel solution.[5] Let

$$a = \gamma(kc - 1) - kc \tag{4a}$$

$$b = 2kc - 1 \tag{4b}$$

$$Fm = (aM_i^2 + b)/(aM_e^2 + b) \tag{4c}$$

$$Gm = M_i^2/M_e^2 \tag{4d}$$

$$Hm = [2 + (\gamma - 1)M_e^2]/[2 + (\gamma - 1)M_i^2] \tag{4e}$$

The flow properties across the combustor can then be expressed as

$$T_e/T_i = Fm^{(b-1)/b} Gm^{(1/b)} \tag{5a}$$

$$T_{t_e}/T_{t_i} = (T_e/T_i)Hm \tag{5b}$$

$$p_e/p_i = Fm^{\gamma(ke-1)/a} \tag{5c}$$

$$p_{t_e}/p_{t_i} = (p_e/p_i)Hm^{\gamma/(\gamma-1)} \tag{5d}$$

$$A_e/A_i = Fm^{-kc(1/a+1/b)} Gm^{kc/b} \tag{5e}$$

$$u_e/u_i = (Fm/Gm)^{(kc-1)/b} \tag{5f}$$

For combustor design analysis, the inlet flow properties, fuel-flow rate, and heat input are usually specified to solve for the exit Mach number. Since the exit Mach number is an implicit parameter in Eq. (5), an iteration technique is required to evaluate the exit Mach number as a function of total temperature ratio and/or area ratio. For a given T_{t_e}/T_{t_i} or A_e/A_i, the corresponding M_e can be found by the Newton-Raphson iteration process as given below. Let

$$F = F_0 - F_1 \tag{6a}$$

$$F_1 = Fm^{\alpha}\, Gm^{\beta}\, Hm^{\Gamma} \tag{6b}$$

$$\frac{dF_1}{dM_e^2} = F_1\left[\frac{a\alpha}{(aM_e^2 + b)} + \frac{\beta}{M_e^2} + \frac{\Gamma(\gamma - 1)}{2 + (\gamma - 1)M_e^2}\right] \tag{6c}$$

$$M_{ej}^2 = M_{e_{j-1}}^2 - \left(\frac{F}{dF_1/dM_e^2}\right)_{j-1} \tag{6d}$$

for the jth iteration, where for a prescribed T_{t_e}/T_{t_i},

$$F_0 = T_{t_e}/T_{t_i} \tag{7a}$$

$$\alpha = 1 - 1/b \tag{7b}$$

$$\beta = 1/b \tag{7c}$$

$$\Gamma = 1 \tag{7d}$$

and for a prescribed A_e/A_i,

$$F_0 = A_e/A_i \tag{7e}$$

$$\alpha = -kc(1/a + 1/b) \tag{7f}$$

$$\beta = kc/b \tag{7g}$$

$$\Gamma = 0 \tag{7h}$$

For engine control, the fuel-flow rate is more convenient to be specified as an independent parameter. The fuel/air mixture ratio will be expressed in terms of a fuel/air equivalence ratio ϕ. Thus the enthalpy flux balance across the combustor determines the required fuel-flow relationship with respect to the required heating value

$$\eta \dot{m}_f H_f = \dot{m}_a(h_{t_e} - h_{t_i}) + \dot{m}_f h_{t_e} \tag{8}$$

For a calorically perfect gas, the following relationships exist:

$$f = \dot{m}_f/\dot{m}_a = \lambda\phi \tag{9}$$

$$h_{t_e} = CpT_{t_e} \quad \text{and} \quad h_{t_i} = CpT_{t_i} \tag{10}$$

The total temperature ratio is finally expressed as Eq. (11) in terms of the engine control parameter ϕ with an assumption that $f \ll 1$

$$T_{t_e}/T_{t_i} = 1 + \lambda\phi Q_f \tag{11}$$

where

$$Q_f = \eta H_f/(CpT_{t_i}) - 1 \tag{12}$$

$$T_{t_i} = T_i[1 + 0.5(\gamma - 1)M_i^2] \tag{13}$$

By knowing the combustor inlet conditions from the forebody analysis, the required M_e and A_e/A_i can be determined by the iteration process [Eqs. (6) and (7)] for a given kc and T_{t_e}/T_{t_i} specified by the fuel-flow rate [Eq. (11)]. Then the combustor exit flow parameters can be calculated as a function of M_e by Eqs. (4) and (5).

Once the combustor geometry is designed for a desired condition, the required area ratio will be fixed for subsequent analysis of any off-design flight condition. For a specified inlet Mach number and fuel-flow rate, the parameter kc is automatically adjusted to satisfy the fixed area ratio requirement.

Finally, the engine thrust that acts in the centerline direction of the divergent channel combustor is defined as

$$Th_p = \dot{m}_i u_i[(u_e/u_i - 1) + fu_e/u_i] + p_i A_i\{[p_e A_e/(p_i A_i)] - 1] + 0.5(p_e/p_i + 1)(A_e/A_i - 1)\} \tag{14}$$

Afterbody Nozzle Analysis

The entire afterbody surface on the under side of the vehicle serves the function of an expansion nozzle in the integrated SCRAMJET vehicle configuration (see Fig. 2). The exhaust gas expands over the afterbody, and integration of the pressure distribution over the surface produces additional

thrust as well as lift and pitching moment. The static pressure decreases with an increasing Prandtl-Meyer expansion angle [Eq. (15)] defined by change in the nozzle deflection angle. However, the nozzle thrust component increases proportionally with tangent of the nozzle deflection angle as given in Eq. (16):

$$p = p(\Delta v) \tag{15}$$

$$Th_n = \int p[\tan(\delta_n)\cos(\alpha) - \sin(\alpha)]\,dx_n \tag{16}$$

$$L_n = \int p[\cos(\alpha) + \tan(\delta_n)\sin(\alpha)]\,dx_n \tag{17}$$

Therefore, the expansion angle of the afterbody nozzle that produces the maximum thrust component in the flight-path direction is defined as the designed nozzle. For simplicity, only a first-order wave interaction is considered. For a two-dimensional expansion flow, the pressure remains constant in the region from the afterbody expansion corner to the point where a leading wave, reflecting off the cowl, intersects the nozzle surface as depicted in Fig. 2. Beyond this point, the pressure decay is simulated by the area ratio expansion. For a nozzle flow started by the divergent area combustor, a two-dimensional fan-like flowfield is assumed in calculation of the surface pressure distribution.

Propulsive Force Components and Specific Impulse

The engine thrust produced by the combustor has been given by Eq. (14), and the secondary thrust, lift, and pitching moment induced by the afterbody were discussed in the previous section. The total net propulsive force components, defined in *the flight-path coordinate system*, are obtained by summing the combustor and the afterbody nozzle forces. The force and moment coefficients are defined with respect to *the combustor inlet area per width of engine module:*

$$Ct_p = Th/(q_\infty A_i) \tag{18}$$

$$Cl_p = L/(q_\infty A_i) \tag{19}$$

$$Cm_p = M/(q_\infty A_i L B_f) \tag{20}$$

The specific impulse is defined by dividing the thrust component oriented in the flight-path direction by the fuel mass flow. This definition is slightly different from the standard convention in which the specific impulse is usually computed with respect to the total propulsive force generated by the engine including the induced thrust and lift components:

$$ISP(s) = Th/(g\dot{m}_f) \tag{21}$$

External Aerodynamic Force Components

For a generic hypersonic vehicle with a flat top surface, the aerodynamic forces induced by the leeward surface are considered negligible. However, in reality, the aerodynamic contributions induced by the nonflat upper vehicle components should be included. For the present analysis, the aerodynamic contributions are derived from the forces on the lower forebody surface and the external cowl, which are not included in the definition of the propulsive forces.

Good acceleration capability is a prime consideration in the design of a hypersonic vehicle such as the National Aerospace Plane, whose ultimate mission is to achieve Earth orbit. The efficiency with which the vehicle accelerates is strongly dependent upon its drag characteristics. In this case, the effective *ISP* is reduced by the drag/thrust ratio as

$$ISP_{\text{eff}} = ISP(1 - D/Th) \tag{22}$$

For this purpose, a reduced angle-of-attack flight or/and a slender forebody configuration improves the total fuel consumption. On the other hand, the thrust may be reduced by capturing a smaller mass flow. This results in a lower thrust loading (Th/W) that may extend the endo-atmospheric flight time, which in turn would increase the total aerodynamic heat load.

It is often quoted in the literature that SCRAMJET performance analysis should be conducted along a constant dynamics pressure flight path, for example, $q_\infty = 71{,}820$ Pa (1500 psf).[4] However, the imposed aeroheating rate is proportional to the cube of velocity so that the heating rate increases proportionally with the velocity along a constant dynamic pressure flight path. In this case, the heating rate becomes unacceptable at upper Mach numbers. For flight in the constant heating rate corridor, the SCRAMJET performance drops off proportionally with increasing altitude. Therefore, a considerable amount of tradeoff study is required to design a viable system. The present methodology permits us to conduct these tradeoff studies quickly and economically.

Hypersonic Viscous Flow Interaction on Forebody Inlet

The analyses discussed in the previous sections are conducted with an inviscid flowfield. However, one of the most important phenomena that cannot be ignored is the hypersonic viscous interaction (VI) effect. A prediction methodology based on a second-order weak interaction theory[7] for an adiabatic wall is used to assess the VI influence.

In the region where the hypersonic viscous flow interaction parameter $\bar{\chi}$ is approximately less than 3.5, the boundary-layer growth because of the VI can be estimated by a second-order weak interaction theory. This theory may be applied for a flow over the forebody surface with an angle of attack, provided the VI computation is based on the local flow properties. A strong VI exists in the neighborhood of a sharp nose. Also the VI effects become more pronounced with increasing Mach number and altitude. As a consequence, the thickness of the boundary layer on the forebody in the vicinity of the combustor inlet may become the same order of magnitude as the inlet height. This may reduce the operational effectiveness of the SCRAMJET concept at a high Mach number and high altitude flight.

Effect of Variable Specific Heat Ratio

It is anticipated that high-enthalpy flow will be encountered during SCRAMJET operation. The heated air is expected to exhibit calorically imperfect, real-gas behavior. In order to assess the order of magnitude influence on SCRAMJET performance, the real-gas effect is simulated by considering a variable specific heat ratio. For simplicity, the specific heat ratio is varied as a function of local temperatures immediately downstream of each shock on the forebody and heat addition in the combustor.

Discussion of Sample Results

Design and Off-Design Comparison

The design condition is usually established by the highest Mach number in the anticipated hypersonic flight corridor. The off-design flight Mach number is then taken below the design point so that shock wave ingestion can be avoided at the cowl lip. Also aerodynamic heating must be controlled. To do this, altitudes are usually assigned so that dynamic pressure is decreased with an increasing Mach number, but where the vehicle can still generate sufficient lift for ascending flight. For an accelerating system, a flight path with small angles of attack should be chosen for the best fuel efficiency. For hypersonic cruise, a trimmed AOA attitude that produces the maximum lift over drag ratio $[(L/D)_{\max}]$ should be selected. However, it must be noted that an acceleration leg that consumes a substantial portion of the fuel is always required to reach the hypersonic cruise conditions.

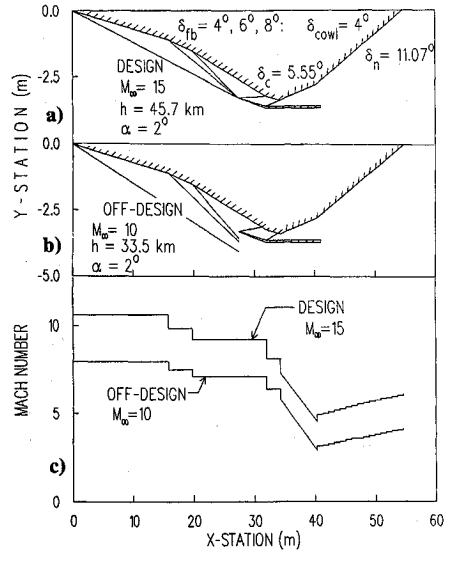

Fig. 3 Sample design and off-design comparison: a) design configuration and shock patterns; b) off-design shock patterns; and c) design/off-design Mach number distributions.

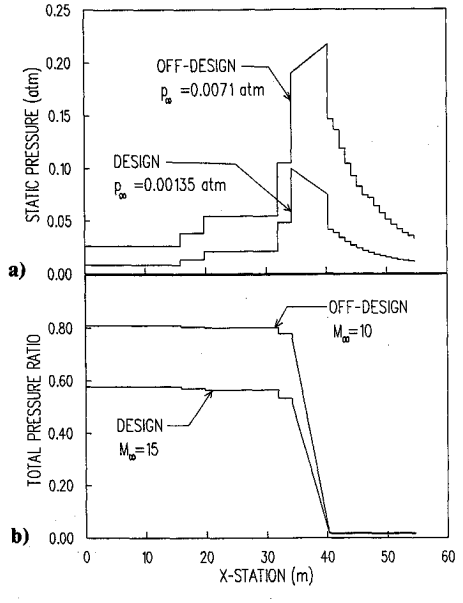

Fig. 4 Design/off-design: a) static pressure distributions and b) total pressure distributions.

For the sample calculation, the design flight condition at $M = 15$, AOA = 2 deg, and $h = 45.72$ km (150,000 ft) was selected and liquid hydrogen fuel (LH_2) used as the fuel. The forebody geometry and shock patterns for the design are shown in Fig. 3a. The vertical scale is magnified to give a detailed depiction of the underbody geometry. The 100% captured mass flux is 11.4 kg/s per unit width of engine. The combustor and the afterbody geometries are designed for a $kc = 1.2$ and for a $\phi = 1.2$, which is a slightly fuel rich condition. Two factors were considered for selecting a $\phi = 1.2$: 1) the primary reason is to obtain higher thrust and 2) the active cooling system using LH_2 may necessitate more coolant flow rate than the engine requires for the stoichiometric combustion. The combustor length of 6.1 m (20 ft) is estimated by considering the fuel reaction time and the air flow velocity in the combustor. The afterbody deflection angle is expanded to 11.07 deg. This provides the maximum design thrust in the flight-path direction.

An off-design performance is computed at $M = 10$, AOA = 2 deg, and $h = 33.5$ km (110,000 ft). As observed in Fig. 3b, the shocks become detached from the cowl lip. The captured mass flux is reduced to 0.525 of the freestream, but the net mass flux of 22.5 kg/s is greater than that for the design condition because the vehicle is flown at a lower altitude.

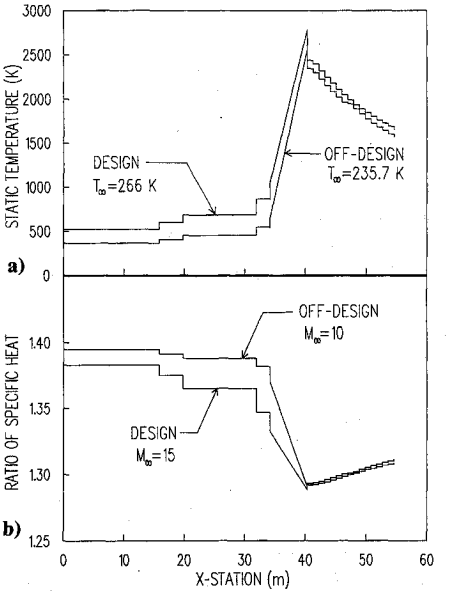

Fig. 5 Design/off-design: a) static temperature distributions and b) ratio of specific heat ratio distributions.

The longitudinal distributions of flowfield properties are compared for the design and off-design conditions. The Mach number distributions (see Fig. 3c) indicate that hypersonic flows enter the combustor. The absolute static pressure (see Fig. 4a) at the combustor inlet is approximately 0.1 atmosphere for the design. The higher pressure environment of 0.2 atm for the off-design case may ease the combustion process. The total pressure ratio (see Fig. 4b) shows that more than 40% of the total pressure loss across the initial bow shock wave occurs for the design condition. The total pressure loss across the bow shock improves for an off-design condition because of the lower flight Mach number. High penalty for the total pressure loss is paid in the supersonic combustion.

The peak temperatures which are approximately 2800 K and 2600 K for the design and off-design conditions, respectively, occur at the combustor exit (see Fig. 5a). The ideal gas approximation is expected to be invalidated by the dissociation of air/gas at these elevated temperatures. The resulting distributions of the ratio of specific heat (see Fig. 5b) indicate that the real-gas effect is more pronounced for the design condition.

Comparison with Varying Design Point Mach Numbers

To demonstrate versatility of the present methodology, the changes that occur in vehicle geometry and performance with varying design point Mach numbers are investigated. For this demonstration, AOA, forebody ramp angles, and length from the nose to the cowl lip are fixed. The design cases are for $M = 8$ at $h = 30.5$ km (see Fig. 6a); $M = 12.5$ at $h = 38.1$ km (see Fig. 6b); and $M = 20$ at $h = 61$ km (see Fig. 6c). Qualitatively, the following changes are observed with an increasing design Mach number: 1) the positions of the second and third ramps shift in backward direction; 2) the vehicle slenderness ratio decreases; 3) the combustion inlet area is reduced; 4) the percentage reduction in effective *ISP* becomes worse; and 5) the net thrust decreases because of smaller combustor inlet area and lower dynamic pressure.

The foregoing results have demonstrated that an *ISP* advantage of the SCRAMJET exists over a rocket propulsion system at $M = 20$ and $h = 61$ km. However, the absolute thrust level may become insufficient to provide an efficient

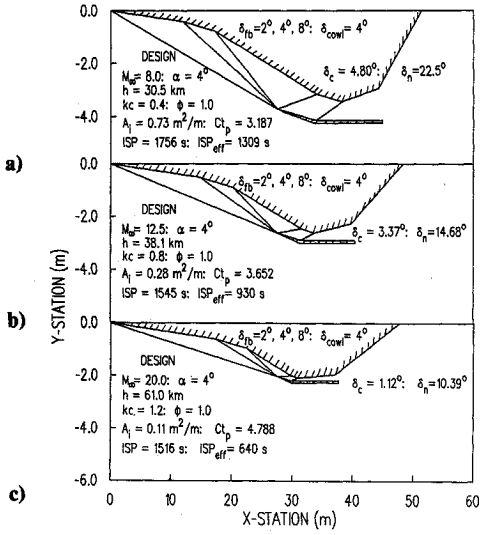

Fig. 6 Geometry/performance comparisons with design point Mach numbers: a) $M_\infty = 8$, $h = 30.5$ km; b) $M_\infty = 12.5$, $h = 38.1$ km; and c) $M_\infty = 20$, $h = 61$ km.

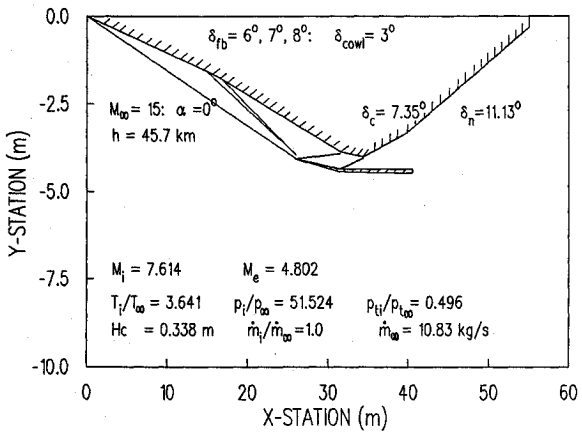

Fig. 7 Generic integrated SCRAMJET vehicle for performance analysis.

acceleration system. The attractiveness of the SCRAMJET in the low acceleration environment may diminish rapidly especially when the complex design and the weight penalty arising from the thermal protection system and a poor volumetric efficiency of LH_2 are considered.

Propulsion Performance Data for Integrated SCRAMJET Vehicle

A typical set of propulsion performance data (thrust, lift, and pitching moment coefficients and specific impulse) are generated for the integrated SCRAMJET vehicle during accleration from $M_\infty = 10$ at $h = 32$ km (105,000 ft) to $M_\infty = 15$ at $h = 45.7$ km (150,000 ft). The generic configuration is shown in Fig. 7. The design point has been selected at $M_\infty = 15.5$, AOA = 2 deg, and $h = 48.8$ km (160,000 ft) in order to expand the operational capability at $M_\infty = 15$. The initial forebody wedge angle is selected to be 6 deg in order to increase the absolute thrust for acceleration. A combustor efficiency η is assumed to be 0.6 to account for uncertainties in mixing/combustion processes, etc. A variable specific heat ratio option is applied.

The parametric plots of lift coefficient vs thrust coefficient are shown in Fig. 8. The AOA and the fuel/air equivalence ratio are used as the independent parameters. In all cases, thrust coefficients vary almost linearly with lift coefficients for constant AOA. Nonlinear responses of coefficients to change

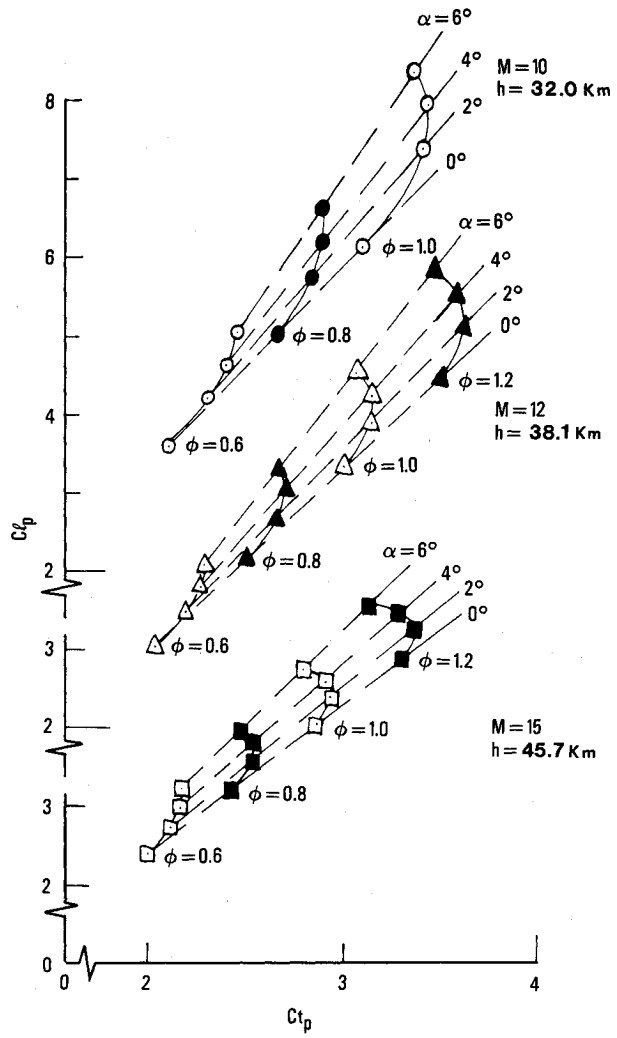

Fig. 8 SCRAMJET propulsive lift vs thrust coefficients (flight-path coordinate).

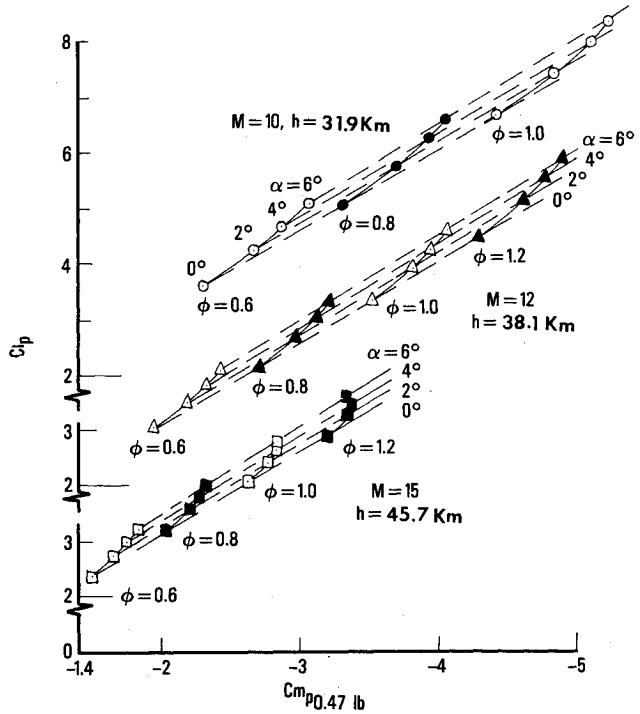

Fig. 9 SCRAMJET propulsive lift vs pitching moment coefficients (flight-path coordinate).

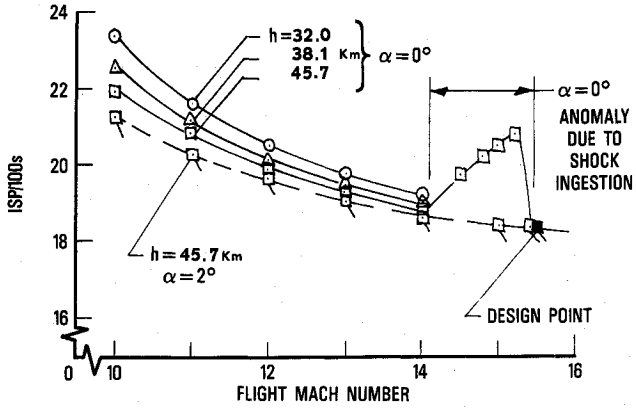

Fig. 10 SCRAMJET specific impulse vs flight Mach number, $\phi = 1$.

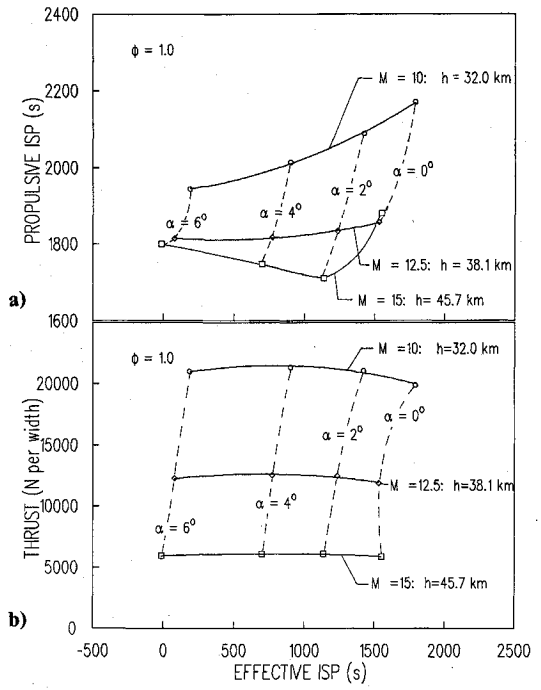

Fig. 11 Effective *ISP* vs a) propulsive *ISP* and b) absolute thrust, $\phi = 1$.

in AOA are observed with constant fuel-flow settings. The regions of applicability at a given fuel setting expand with decreasing Mach number operations.

The static stability plots of lift coefficients vs pitching moment coefficients are shown in Fig. 9. The moment reference is taken at the 47% point of the vehicle longitudinal station and on the vehicle upper surface. Similar qualitative trends to those shown in Fig. 8 are observed in Fig. 9. For a given flight attitude, i.e., fixed Mach number and angle of attack, this observation implies that sufficient control power exists with the fuel-flow settings used here.

The variation of specific impulse with Mach number is shown in Fig. 10. The system *ISP* is greater than 1800 s. This is considerably better than the system *ISP* of LH_2 rocket, which is approximately 450 s. The level of *ISP* is found to depend on altitude and angle of attack as well as Mach number. For an AOA = 0 deg, an anomalous rise in the *ISP* appears between $14 < M_\infty < 15.5$. This anomaly is produced because the vehicle's forebody was designed intentionally for $M_\infty = 15.5$ and AOA = 2 deg. Thus, a shock ingestion occurs for off-design flight conditions where the AOA is less than 2 deg in the Mach number range noted above. This conjecture is confirmed by the AOA = 2 deg curve that depicts a smooth decay in *ISP* with increasing Mach number. The effect of shock ingestion does not appear noticeably in the thrust coefficient of Fig. 8 because the increase in mass flux by the ingested shock has influenced both the thrust and lift coefficients. A similar anomalous trend is detected in the thrust coefficient vs Mach number plot, but this plot is not shown.

For an accelerating system, the measure of fuel efficiency can be dictated by the effective *ISP* [Eq. (22)] and not by the system *ISP* alone. The propulsive *ISP* vs effective *ISP* are plotted in Fig. 11a for $\phi = 1$. The drag of the forebody and external cowl are computed at several AOA between 0 and 6 deg. For the flight conditions examined, the effective *ISP*s reduce rapidly with increasing AOA. The implication of this trend is that an accelerating vehicle should be operated at reduced AOA for fuel efficiency. This finding was also noted by Small et al.[4]

Another consideration required in the performance analysis of an accelerating SCRAMJET vehicle is that the flight time in the severe aeroheating environment is greatly affected by the vehicle's thrust-to-weight ratio (Th/W). A plot of absolute thrust per unit engine width vs effective *ISP* is shown in Fig. 11b. The thrust at $M_\infty = 15$ is reduced to approximately 1/4 of the value at $M_\infty = 10$, due to the higher operating altitude. In other words, a vehicle with higher *ISP* but with lower thrust loading prolongs the flight time in order to achieve the same required energy level for its mission. In this case, the *ISP* advantage can be offset by the increasing structure weight, which may be necessitated by the lengthy soaking time of the aeroheating load.

Effect of Viscous Interaction on Forebody

The boundary-layer displacement thickness distributions computed on an adiabatic wall with hypersonic VI are shown in Fig. 12. The boundary-layer displacement thickness exceeds 0.3 m as it approaches the inlet at $M_\infty = 20$ and $h = 61$ km. The inlet height is in the same order of magnitude as the boundary-layer displacement thickness as can be scaled from Fig. 6c. The mass flow in the combustor section is, therefore, highly restricted because the effective shape of the forebody surface is changed by the reduced mass flux within the boundary layer. The displacement thicknesses are substantially thinner for the $M_\infty = 15$ and 10 flight conditions. The two factors that contribute to the observed thickness reductions are 1) a decrease in Mach number and 2) an increase in the unit Reynolds number due to lower operational altitude.

Recommendations for Future Improvements

The following modifications should be included in the forebody computational methodology: 1) iteration of the shock strength that accounts for the proper specific heat ratio jump; 2) the viscous interaction effect on a nonadiabatic wall, which is expected to reduce the boundary-layer displacement thickness growth; and 3) the three-dimensional forebody effect that can be corrected by estimating the initial bow shock and treating the subsequent downstream flowfield by the hypersonic strip theory. The boundary-layer growth should be included in the flow analysis of the combustor and the afterbody nozzle to properly account for the viscous drag.

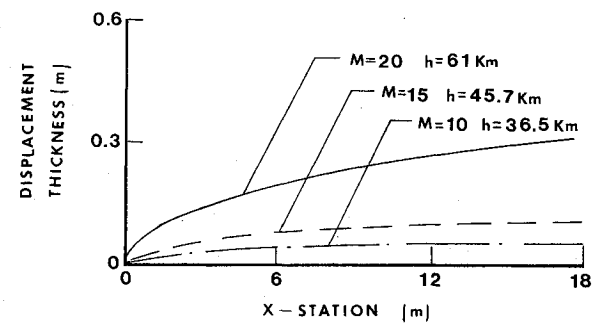

Fig. 12 Viscous interaction effect: forebody boundary-layer displacement thickness.

Conclusion

A simplified methodology for design and performance prediction of an integrated SCRAMJET vehicle is developed, which is intended to be used for a preliminary design analysis. Specifically, a set of close-form solutions for analyzing the divergent area supersonic combustor is derived by introducing a kc parameter that relates the area gradient and heat input. To control the engine throttling, the fuel/air equivalence ratio is used as an independent parameter. The present methodology 1) offers an insight to enhance the understanding of the integrated SCRAMJET vehicle performance, 2) allows rapid evaluations of a design concept, and 3) generates the performance trend data for trade-off study. Because this methodology is based on ideal conditions, it may produce more optimistic results as compared to the real case. However, qualitatively realistic trends of the system performance for an integrated SCRAMJET vehicle are expected. It should be noted that this methodology does not claim to conduct detailed SCRAMJET analysis, a capability that depends upon CFD research.

Acknowledgment

The development of methodology was funded by a Northrop Independent Research & Development project. Portions of the data presented were generated for the Robust Control Law Development for Modern Aerospace Vehicle Contract F33615-87-C-3606 under the sponsorship of the Air Force Flight Dynamics Laboratory. The author expresses his appreciation to H. Gerhardt and D. L. Antani (presently at McDonnell-Douglas) of Northrop for the motivation to pursue this project.

References

[1]White, M. E., Drummond, J. P., Kumar, A., "Evolution and Application of CFD Technique for SCRAMJET Engine Analysis," *Journal of Propulsion*, Vol. 3, No. 5, Sept.–Oct. 1987, pp. 423–438.

[2]Sinha, N., and Dash, S. M., "Parabolized Navier-Stokes Analysis of Ducted Supersonic Combustion Problems," *Journal of Propulsion*, Vol. 3, No. 5, Sept.–Oct. 1987, pp. 455–464.

[3]Rizkalla, O., Chinitz, W., and Erdos, J. I., "Calculated Chemical and Vibrational Nonequilibrium Effects in NASP-Type Nozzles," AIAA Paper 88-3263, July 1988.

[4]Small, W. J., Weidner, J. P., and Johnston, P. J., "SCRAMJET Nozzle Design and Analysis as Applied to Highly Integrated Hypersonic Research Airplane," NASA TN-D-8334, Nov. 1976.

[5]Oates, G. C. (ed.), *Aerothermodynamics of Aircraft Engine Components*, AIAA Education Series, New York, 1985, pp. 97–104.

[6]Kerrebrock, J. L., *Aircraft Engines and Gas Turbines*, The MIT Press, Cambridge, MA, 1983, pp. 255–257.

[7]Kubota, T., and Ko, D. R. S., "A Second-Order Weak Interaction Expansion for Moderately Hypersonic Flow Past a Flat Plate," *AIAA Journal*, Vol. 5, No. 10, Oct. 1967, pp. 1915–1917.